

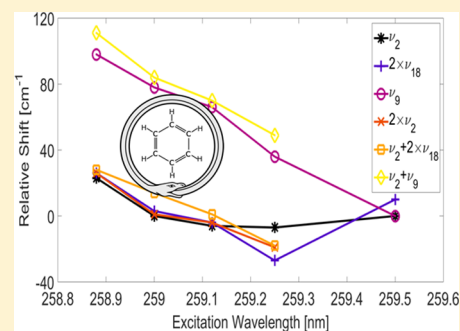
Resonance-Enhanced Raman Scattering of Ring-Involved Vibrational Modes in the ${}^1B_{2u}$ Absorption Band of Benzene, Including the Kekule Vibrational Modes ν_9 and ν_{10}

Adam H. Willitsford,^{†,§} C. Todd Chadwick,[‡] Stewart Kurtz,[†] C. Russell Philbrick,^{†,‡} and Hans Hallen^{*,‡}

[†]The Pennsylvania State University, School of Electrical Engineering and Computer Science, State College, Pennsylvania 16802, United States

[‡]The North Carolina State University, Department of Physics, Raleigh, North Carolina 27695-8202, United States

ABSTRACT: Resonance Raman spectroscopy provides much stronger Raman signal levels than its off-resonant counterpart and adds selectivity by excitation tuning. Raman preresonance of benzene has been well studied. On-resonance studies, especially at phonon-allowed absorptions, have received less attention. In this case, we observe resonance of many of the vibration modes associated motion of the carbons in the ring while tuning over the ${}^1B_{2u}$ absorption, including the related ν_9 (CC stretch Herzberg notation, ν_{14} Wilson notation) and ν_{10} (CH-parallel bend Herzberg notation, ν_{15} Wilson notation) vibrational modes along with the ν_2 (CC-stretch or ring-breathing Herzberg notation, ν_1 Wilson notation) mode and multiples of the ν_{18} (CCC-parallel bend Herzberg notation, ν_6 Wilson notation) vibrational mode. The ring-breathing mode is found to mix with the b_{2u} modes creating higher frequency composites. Through the use of an optical parametric oscillator (OPO) to tune through the ${}^1B_{2u}$ absorption band of liquid benzene, a stiffening (increase in energy) of the vibrational modes is observed as the excitation wavelength nears the ${}^1B_{2u}$ absorption peak of the isolated molecule (vapor) phase. The strongest resonance amplitude observed is in the $2 \times \nu_{18}$ (e_{2g}) mode, with nearly twice the intensity of the ring-breathing mode, ν_2 . Several overtones and combination modes, especially with ν_2 (a_{1g}), are also observed to resonate. Raman resonances on phonon-allowed excitations are narrow and permit the measurement of vibrations not Raman-active in the ground state.



INTRODUCTION

Resonance enhancements of the benzene Raman signals are presented, and they show significant enhancements when tuning over the vapor (isolated molecule) absorption peaks. Many previous studies have investigated resonance Raman in benzene but lacked the fine-tuning of the excitation wavelength that is used in this study.^{1–4} Ziegler and Hudson¹ made measurements of the near-resonance enhancement of liquid benzene diluted to 1% in acetonitrile by using a 212.8 nm excitation to probe the singlet (${}^1B_{1u}$) transition. The spectra measured here are believed to be the first resonance-enhanced Raman spectra measured, where fine resolution tuning (0.25 nm steps) of the excitation wavelength reveals significant changes in the Raman modes of benzene.⁵ These results show that the only fundamental enhanced mode is the ν_2 992 cm^{-1} ; note that Herzberg notation is used throughout the balance of this paper.⁶ Furthermore, the overtone and combinational modes that result stem from the e_{2g} state. Asher and Johnson² performed measurements of the resonance enhancement of benzene by using ~ 2 nm steps in the range 220–251 nm through the absorption bands of liquid benzene and measuring the 992 cm^{-1} peak relative to the acetonitrile peak at 918 cm^{-1} . Gerrity et al.³ probed benzene vapor in the deep ultraviolet, confirming the ν_2 (992 cm^{-1}) enhancement as well as the e_{2g} combinational and overtones. Sension et al.⁴ recorded resonance-enhanced Raman spectra of benzene in the ${}^1B_{1u}$

region, and again the spectra also show the enhancement of the e_{2g} modes of vibration together with the enhanced fundamental ν_2 . Here we present a detailed description of the Raman spectra for excitation wavelengths scanning through ${}^1B_{2u}$ absorption band with a focus on the absorption peak near 259 nm. As previously reported,⁵ the peak in the resonance response is observed to coincide with the vapor phase absorption peaks.^{7,8} The results of our Raman spectra show not only enhancement of the fundamental ν_2 (993 cm^{-1}) vibration and at multiples of the ν_{18} (608 cm^{-1}) vibration but also enhancements of the dipole-forbidden Kekule ν_9 (1309 cm^{-1}) and ν_{10} (1150 cm^{-1}) b_{2u} vibrational modes. As the excitation wavelength is scanned closer to the absorption peak, a major increase in stiffening of ν_9 is observed; it is interesting that this feature is found in the calculations and modeling performed by Haas and Zilberg.⁹

EXPERIMENTAL SECTION

An optical parametric oscillator (U-Oplaz) pumped by the third harmonic of a Nd:YAG laser (Spectra Physics) is used to produce a continuously tunable output from approximately 420 to 710 nm. Frequency-doubling the OPO output with a β -BBO

Received: August 21, 2015

Revised: December 27, 2015

crystal generates the excitation source, with an ultraviolet tuning range from ~ 210 to 355 nm. The excitation laser maintained an average output power of 1 to 2 mW while scanning through a wide range of ultraviolet wavelengths and operated with a 7 ns pulse width and 10 Hz pulse repetition. The OPO cavity uses a type-1 BBO crystal to generate a tunable signal with a bandwidth of approximately 40 cm^{-1} at 260 nm. The laser flux densities are kept below 1 mJ/cm^2 to avoid saturation effects.¹⁰ The laser beam diameter of 0.8 cm typically provided an average energy density of ~ 0.4 mJ/cm^2 for the measurements described here. The Teflon sample cell at 45° to the incident beam uses fused silica windows mounted for a 90° scattering geometry. The scattered light was collected with a lens system and focused into a Jobin Yvon Spex Triplemate 1877 spectrometer with a 2400 gr/mm grating blazed at 250 nm. The Raman scattered lines are imaged onto an Andor back illuminated UV-enhanced EM-CCD (Electron Multiplying-CCD) detector. Integration times of 1 to 2 min were typically used to achieve well-defined Raman signatures with typical signal-to-noise ratios of 5 to 15 . The CCD camera configuration permitted a detection field-of-view corresponding to ~ 5.7 nm. The type-1 OPO generator of the tunable laser beam resulted in a relatively large line width; the resolution of the system is ~ 0.25 nm (40 cm^{-1}) at 260 nm. Additional details of the experimental setup have been previously discussed.⁵

RESULTS AND DISCUSSION

The fundamental ν_2 (993 cm^{-1}), ν_9 (1309 cm^{-1}), ν_{10} (1150 cm^{-1}), and second multiple of ν_{18} (608 cm^{-1}) vibrational modes^{11,12} are resonantly enhanced and energy shifted to ν_2 (1014 cm^{-1}), ν_9 (1407 cm^{-1}), ν_{10} (1210 cm^{-1}), and $2 \times \nu_{18}$ (1238 cm^{-1}) as the wavelength of excitation is tuned through vapor-phase absorption peak near 259 nm. Three of these are strong and observed as separate peaks, while the ν_{10} appears as a shoulder to the left of the larger $2 \times \nu_{18}$ peak. There is some evidence for additional peaks near 1550 and 1700 cm^{-1} , perhaps including $\nu_2 + \nu_{18}$, but the signal-to-noise is poor enough that we do not pursue them further. The assignments are discussed below. Each spectrum has been processed to remove background, normalized to remove the generic Raman scattering cross section, ν^4 dependence, and corrected for changes in laser power as a function of tuning wavelength. The resonance enhanced Raman spectra at four excitation wavelengths near the vapor-phase absorption maxima at 259 nm are shown in Figure 1.

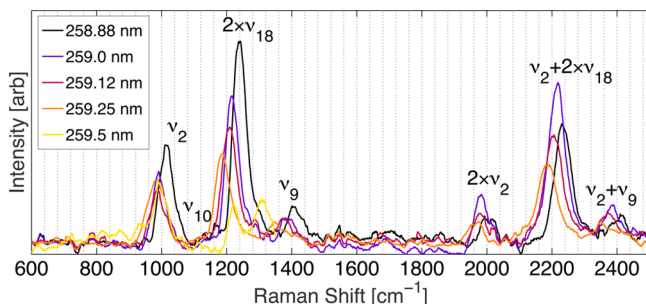


Figure 1. Resonance-enhanced Raman scatter from liquid benzene. The ring-breathing mode (ν_2) as well as ν_9 and ν_{10} are found to be resonantly enhanced as the excitation wavelength is tuned through the highly structured vapor-phase absorption peak.

At resonance, the ring-breathing mode, ν_2 , is found to mix with itself (first-harmonic), $2 \times \nu_{18}$ mode, and the b_{2u} modes repeating the triplet (with shoulder on central peak) and is shown in Figure 1 starting at ~ 2000 cm^{-1} . The strong activity of the ν_2 mode is due to its relation to the absorption, which results in a weakening of the ring bonding. This vibrational mode also forms the basis for the strong absorption near 259 nm in this phonon-allowed absorption manifold. The resonant excitation is strongly absorbed into the ring-breathing mode, creating distortions in the carbon bonding. In fact, all resonantly enhanced vibration modes include motions that involve the carbon atoms of the ring. Whether all vibrations that involve such motions are resonant is harder to determine because ν_6 (CCC-parallel bend at 1010 cm^{-1}) would be hidden by the strong ring stretching response and $2 \times \nu_8$ (CCC-perpendicular bend at 703 cm^{-1}), also Raman forbidden, could be mixed into the ν_9 peak. The presence of the normally Raman-forbidden Kekule modes is somewhat surprising and may result from the absorption-induced distortion of the Kekule ring present in the b_{2u} symmetry. In such a case, the Raman intensity related to these modes would be expected to decrease dramatically as the excitation is tuned away from the resonance energy; however, the intensity of these lines in Figure 1 is observed to decrease at about the same rate as the other, normally Raman-allowed, resonantly enhanced lines. Another possible explanation of these results can be found in the π -avoided crossing model, which can account for the origins of the low skeletal b_{2u} frequencies ν_9 and ν_{10} in the ground state and its Duschinsky mode mixing with the b_{2u} rocking vibration ν_{18} resulting in the state selective frequency exaltation of ν_9 .¹³

A comparison of the two “triplets” shown in Figure 1, the second shifted by the energy of ν_2 , indicates a slight shift in the excitation wavelength that produces the maximum resonance gain, by ~ 0.1 nm, as the ν_2 mode is combined with the fundamental “triplet”. This reduction in the resonance energy could relate to anharmonicity. It is odd that the stiffening of the modes remains unchanged, with the largest vibration energy shift occurring at the same excitation wavelength as both the maximum resonance gain and peak shift of the fundamental “triplet”. The maximum enhancement returns to the excitation wavelength of the fundamental “triplet” when the “triplet” is shifted by the energy of $2 \times \nu_2$ (not shown).

A comparison of the resonant (258.88 nm) and nonresonant (430 nm) Raman spectra recorded is shown in Figure 2, with the modal “triplet” seen again after mixing with the multiples of the ring breathing (ν_2 , $2\nu_2$) vibrational mode. It is also evident that the ν_1 (CH-stretch) mode is not resonantly enhanced. This is likely due to the fact that bonding of the hydrogen atoms to the ring is not strongly impacted by changes to the ring backbone; that is, this vibration does not alter the ring. The spectra have not been corrected for self-absorption effects. The correction for the absorption due to the liquid benzene with 258.88 nm excitation accounts for the approximately $1000\times$ fewer molecules than contribute relative to the visible Raman spectrum. Therefore, the scattering cross section in $\text{cm}^2/\text{molecule}$ at resonance must be $\sim 1000\times$ larger.

The shifting of the peaks, as the vibrations move from the energies in the ground state to those in the excited state on resonance, complicates the assignment of peaks to vibration modes. The relatively broad energy width of the tunable excitation laser used can cause two nearby peaks to merge into one, as noted above. The most accurate method to resolve this problem is to plot the energy shift from known vibration

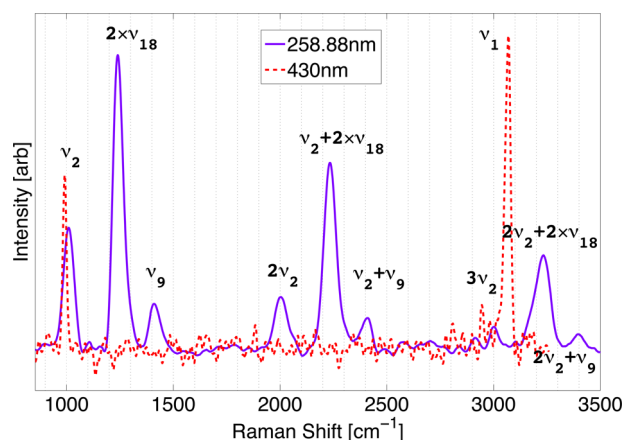


Figure 2. Benzene resonant (258.88 nm) and nonresonant (430 nm) Raman spectra. The spectra have not been corrected for self-absorption effects.

energies as a function of the excitation wavelength as it moves away from the resonance. If the shift from the reference value approaches zero far from resonance, then the assignment is likely correct. The width of the peak does not matter unless more than one vibration mode contributes to it, in which case the line may approach a weighted average of their energies. The plot in Figure 1 also provides a clear presentation of the stiffening of the vibration modes as resonance is approached, and this feature is more clearly shown in Figure 3. With the chosen assignments, all peak shifts do approach zero away from resonance, which is strong evidence of their correctness.

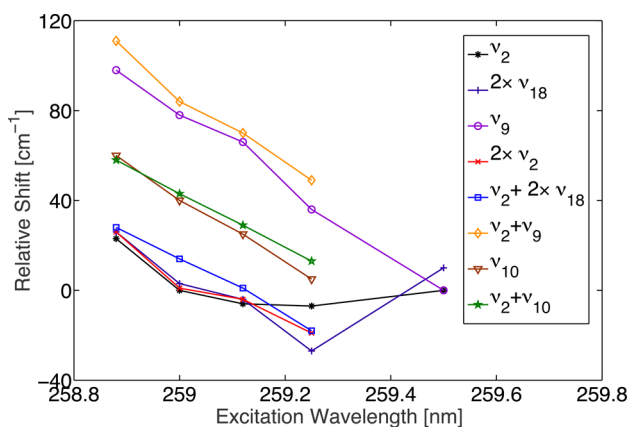


Figure 3. Peak positions of the Raman peaks in Figure 1 are plotted relative to their nominal, off resonance positions to show the stiffening of the vibrations as the 258.88 nm resonance is approached.

Most of the modes are found to stiffen similarly as resonance is approached. Several are observed to have a slight weakening (negative values) compared with the reference (visible, off resonance) wavelength data and exhibit stiffening as resonance is approached. The ν_9 mode and its combination with ν_2 are similar to each other but quite different from the others, as found in Hass and Zilberg⁹ and Shaik et al.¹³ Second, the modes involving ν_9 are found to be more linear. Apparently, the elastic landscape does not uniformly adjust as the excited state is approached—symmetry plays a large role as found in Ohno and Takahashi.¹⁴ As a numerical example, the ν_9 and $2 \times \nu_{18}$ vibrational modes in the ground state are found at ~ 1309 and

1216 cm^{-1} , respectively; here in the resonantly enhanced excited state they are found at 1407 and 1238 cm^{-1} . Indications of the peak shifts are observed in Figure 1, and the dependence is plotted in Figure 3. The shift in ν_9 is about five times larger than the shift in $2 \times \nu_{18}$. The large stiffening of ν_9 and the mode selectivity as the excitation wavelength is moved closer to the peak of the isolated molecule absorption were predicted by Haas and Zilberg.⁹ This shift is found to be $\sim 100 \text{ cm}^{-1}$ (ν_9 to 1407 cm^{-1}), and it is considerably smaller than the ν_9 vibration shift to $\sim 1566 \text{ cm}^{-1}$ seen in two-photon spectroscopy^{15–19} and MO calculations.²⁰ This could be due to imperfect match of the laser wavelength or the large bandwidth of the laser source with respect to the isolated molecule absorption peak in benzene. Additionally, these data show the strong vibronic coupling of the b_{2u} modes between the $^1A_{1g}$ ground state and the $^1B_{2u}$ excited state, further supporting Friedrich and McClain that the vibrational b_{2u} modes receive the majority of their vibrational excitation from the $^1B_{2u}$ excited state.¹⁹

CONCLUSIONS

The ν_2 , ν_{10} , $2 \times \nu_{18}$, and ν_9 vibrational modes in liquid benzene are observed to be resonantly enhanced in a small region of excitation wavelength near the vapor-phase (isolated molecule) absorption at $\sim 259 \text{ nm}$. The b_{2u} (ν_9 and ν_{10}) vibrational modes are observed in the resonance Raman spectra, of which ν_9 exhibits an unusual increase in energy (stiffening) as the laser excitation wavelength is scanned closer to the peak of the isolated molecule (vapor phase) absorption, as demonstrated by the excited state S_1 (B_{2u}) vibrational energy shifts. The vibrational mode energies move closer to those seen in two-photon excitation spectroscopy and may shift even closer with a better match (smaller bandwidth laser) between the laser excitation source and the isolated molecule absorption. This large shift is consistent with that predicted in Shaik et al. in the twin-state avoided crossing model and their ab initio “Lego model” valence bond calculations and full π configuration interaction MO calculations.²¹

AUTHOR INFORMATION

Corresponding Author

*Tel: 919-515-6314. E-mail: hans_hallen@ncsu.edu.

Present Address

§A.W.: Johns Hopkins University - Applied Physics Laboratory, Laurel, MD, 21076.

Funding

The laser source is part of an instrument developed under NSF grant DMR-9975543.

Notes

The authors declare no competing financial interest.

ACKNOWLEDGMENTS

We thank Michigan Aerospace Corporation for the loan of their Andor (EMCCD) camera. We also thank Dr. Arthur Sedlacek and Dr. Sanford Asher for their technical discussions.

REFERENCES

- Ziegler, L.; Hudson, B. Resonance Raman Scattering of Benzene and Benzene- d_6 with 212.8 nm Excitation. *J. Chem. Phys.* **1981**, *74*, 982–992.
- Asher, S.; Johnson, C. UV Resonance Raman Excitation Profile Through the $^1B_{2u}$ State of Benzene. *J. Phys. Chem.* **1985**, *89*, 1375–1379.

- (3) Gerrity, D.; Ziegler, L.; Kelly, P.; Desiderio, R.; Hudson, B. Ultraviolet Resonance Raman Spectroscopy of Benzene Vapor with 220–184 nm Excitation. *J. Chem. Phys.* **1985**, *83*, 3209–3213.
- (4) Sension, R.; Brudzynski, R.; Li, S.; Hudson, B.; Zerbetto, F.; Zgierski, M. Z. Resonance Raman Spectroscopy of the B_{1u} Region of Benzene: Analysis in Terms of Pseudo-Jahn-Teller Distortion. *J. Chem. Phys.* **1992**, *96*, 2617–2628.
- (5) Willitsford, A.; Chadwick, C. T.; Hallen, H.; Kurtz, S.; Philbrick, C. R. Resonance Enhanced Raman Scatter in Liquid Benzene at Vapor-Phase Absorption Peaks. *Opt. Express* **2013**, *21*, 26150–26161.
- (6) Herzberg, G. *Molecular Spectra and Molecular Structure II. Infrared and Raman Spectra of Polyatomic Molecules*; Van Nostrand: Princeton, NJ, 1945.
- (7) Etzkorn, T.; Klotz, B.; Sørensen, S.; Patroescu, I. V.; Barnes, L.; Becker, K. H.; Platt, U. Gas-Phase Absorption Cross Sections of 24 Monocyclic Aromatic Hydrocarbons in the UV and IR Spectral Ranges. *Atmos. Environ.* **1999**, *33*, 525–540.
- (8) Fally, S.; Carleer, M.; Vandaele, A. UV Fourier Transform Absorption Cross-Sections of Benzene, Toluene, meta-, ortho-, and para-Xylene. *J. Quant. Spectrosc. Radiat. Transfer* **2009**, *110*, 766–782.
- (9) Haas, Y.; Zilberg, S. The $\nu_{14}(b_{2u})$ Mode of Benzene in S_0 and S_1 and the Distortive Nature of the π Electron System: Theory and Experiment. *J. Am. Chem. Soc.* **1995**, *117*, 5387–5388.
- (10) Asher, S. *Coal Liquefaction Process Streams Characterization and Evaluation: UV Resonance Raman Studies of Coal Liquid Residuals*; DOE/PC/89883-67 (DE93009669), 1993.
- (11) Herzberg, G. *Molecular Spectra and Molecular Structure II. Infrared and Raman Spectra of Polyatomic Molecules*; Krieger: Malabar, FL, 1991; p 364.
- (12) Berman, J.; Goodman, L. The a_{2g} Mode in Ground State Benzene. *J. Chem. Phys.* **1987**, *87*, 1479–1487.
- (13) Shaik, S.; Shurki, A.; Danovich, D.; Hiberty, P. Origins of the Exalted b_{2u} Frequency in the First Excited State of Benzene. *J. Am. Chem. Soc.* **1996**, *118*, 666–671.
- (14) Ohno, K.; Takahashi, R. Excited-State Vibrations of Benzene and Polycyclic Aromatic Hydrocarbons: Simple Force Field Models Based on Molecular Orbital Characteristics of Hexagonal Carbon Networks. *Chem. Phys. Lett.* **2002**, *356*, 409–422.
- (15) Wunsch, L.; Neusser, H. J.; Schlag, E. W. Two Photon Excitation Spectrum of Benzene and Benzene- d_6 in the Gas Phase: Assignment of Inducing Modes by Hot Band Analysis. *Chem. Phys. Lett.* **1975**, *31*, 433–440.
- (16) Goodman, L.; Berman, J. M.; Ozkabak, A. G. The Benzene Ground State Potential Surface. III. Analysis of b_{2u} Vibrational mode Anharmonicity through Two-Photon Intensity. *J. Chem. Phys.* **1989**, *90*, 2544–2554.
- (17) Rava, R. P.; Goodman, L.; Krogh-Jespersen, K. Vibronic Mechanisms in the Two-Photon Spectrum of Benzene. *J. Chem. Phys.* **1981**, *74*, 273–281.
- (18) Hochstrasser, R. M.; Sung, H. N.; Wessel, J. E. Moderate-Resolution Study of the Two-Photon Spectrum of the $^1B_{2u}$ State of Benzene- h_6 and Benzene- d_6 . *Chem. Phys. Lett.* **1974**, *24*, 7–10.
- (19) Friedrich, D. M.; McClain, W. M. Polarization and Assignment of the Two-Photon Excitation Spectrum of Benzene Vapor. *Chem. Phys. Lett.* **1975**, *32*, 541–549.
- (20) Ohno, K. A Study of Excited-State Molecular Vibrations of Aromatic Hydrocarbons. *Chem. Phys. Lett.* **1979**, *64*, 560–566.
- (21) Shaik, S.; Shurki, A.; Danovich, D.; Hiberty, P. A Different Story of π -Delocalization—The Distortivity of π -Electrons and Its Chemical Manifestations. *Chem. Rev.* **2001**, *101*, 1501–1539.